Photoproduction of vector mesons in the Soft Dipole Pomeron model

E. MARTYNOV[a,b,1], E. PREDAZZI[c,2] and A. PROKUDIN[c,d,3]

(a) Bogolyubov Institute for Theoretical Physics,
National Academy of Sciences of Ukraine,
03143 Kiev-143, Metrologicheskaja 14b, UKRAINE

(b) Institut de physique Bat B5-a
Université de Liège
Sart Tilman B-4000 Liège,
BELGIQUE

(c) Dipartimento di Fisica Teorica,
Università Degli Studi Di Torino,
Via Pietro Giuria 1, 10125 Torino,
ITALY
and
Sezione INFN di Torino,
ITALY

(d) Institute For High Energy Physics,
142281 Protvino, RUSSIA

Exclusive photoproduction of all vector mesons by real and virtual photons is considered in the Soft Dipole Pomeron model. It is emphasized that being the Pomeron in this model a double Regge pole with intercept equal to one, we are led to rising cross-sections but the unitarity bounds are not violated. It is shown that all available data for $\rho, \omega, \varphi, J/\psi$ and Υ in the region of energies $1.7 \leq W \leq 250$ GeV and photon virtualities $0 \leq Q^2 \leq 35$ GeV^2 , including the differential cross-sections in the region of transfer momenta $0 \leq |t| \leq 1.6$ GeV^2, are well described by the model.

1 Introduction

A new precise measurement of J/ψ exclusive photoproduction by ZEUS [1] opens a new window in our understanding of the process and allows us to give more accurate predictions for future experiments.

The key issue of the dataset [1] is the diffractive cone shrinkage observed in J/ψ photoproduction which leads us to consider it a soft rather than pure QCD process so that we can apply the Soft Dipole Pomeron exchange [2] model.

We are improving the model while not changing its main properties such as the universality for all vector mesons and its applicability in a wide energy region. The structure of the amplitude singularities in the j-plane remains also intact but we use a nonlinear Pomeron trajectory in order to describe correctly the behaviour of the differential distributions. The

[1] *E-mail: E.Martynov@guest.ulg.ac.be*
[2] *E-mail: predazzi@to.infn.it*
[3] *E-mail: prokudin@to.infn.it*

use of non-linear trajectories improves, in fact, the analyticity properties of the scattering amplitude. The secondary Reggeons however, are for simplicity, taken directly with their trajectories as determined from the pure hadronic case. The J/ψ elastic cross section is described as due to the soft Pomeron exchange but without unitarity violation.

We utilize the following picture of the interaction: a photon fluctuates into a quark-antiquark pair and as the lifetime of such a fluctuation is quite long (by the uncertainty principle it grows with the beam energy ν as $2\nu/(Q^2 + M_V^2)$ [3]), the proton interacts via Pomeron or secondary Reggeon exchange with this quark-antiquark pair. After the interaction this pair forms a vector meson [4]. The hint is that such an interaction must be very close to that among hadrons and, following the principle of Regge pole theory, that the Pomeron is universal in all hadron-hadron interactions and in all other processes, including DIS, provided we have an appropriate kinematical region for the Regge approach to hold (vacuum quantum numbers exchange is possible). Thus, if Pomeron exchange is possible, then it has the same properties (the form of singularity, position of such a singularity in the J-plane, trajectory etc.) as in hadron-hadron interaction. This is true at least for on shell particles. A real photon ($Q^2 = 0$) is considered it as a hadron (according to the data). For $Q^2 \neq 0$ we assume that no new singularity appears [5]. More precisely, even if we assume a new singularity at $Q^2 \neq 0$, its contribution must be equal to zero for $Q^2 = 0$. Indeed the analysis of the data [6] shows that there is no need for such a new contribution.

The basic diagram is depicted in Figure 1; s and t are the usual Mandelstam variables, $Q^2 = -q^2$ is the virtuality of the photon.

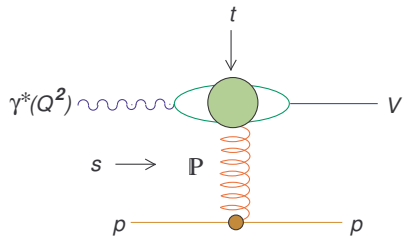

Figure 1: Photoproduction of a vector meson.

It is well known that high-energy representation of the scattering amplitude may be expressed as a sum over the the appropriate Regge poles in the complex j plane [7]

$$A(s,t)_{s\to\infty} \approx \sum_i \eta_i(t)\beta_i(t)(\cos\theta_t)^{\alpha_i(t)}, \tag{1}$$

where $\eta_i(t)$ is the signature factor and θ_t is the scattering angle in the t channel.

In the case of vector meson photoproduction we utilize the variable $z \sim \cos\theta_t$

$$z = \frac{2(W^2 - M_p^2) + t + Q^2 - M_V^2}{\sqrt{(t + Q^2 - M_V^2)^2 + 4M_V^2 Q^2}} \tag{2}$$

where $W^2 = (p+q)^2 \equiv s$, M_V is the vector meson mass, M_p is the proton mass.

Assuming vector meson dominance [8], the relation between the forward cross sections of $\gamma p \to Vp$ and $Vp \to Vp$ is given by

$$\frac{d\sigma}{dt}(t=0)_{\gamma p\to Vp} = \frac{4\pi\alpha}{f_V^2}\frac{d\sigma}{dt}(t=0)_{Vp\to Vp} \tag{3}$$

where the strength of the vector meson coupling $\frac{4\pi}{f_V^2}$ may be found from e^+e^- decay width of vector meson V

$$\Gamma_{V\to e^+e^-} = \frac{\alpha^2}{3}\frac{4\pi}{f_V^2} m_V \tag{4}$$

When $V = \rho_0, \omega, \varphi, J/\Psi$ the relations of these couplings may be obtained assuming SU(4) flavour symmetry. No attempt is made to extend flavour symmetry to SU(5) so as to incorporate also the Υ coupling. The symmetry is too badly broken for this to make sense. Using the quark content of the mesons, we have

$$\begin{aligned} < Q_j^2 >_\rho &= \left|\tfrac{1}{\sqrt{2}}(\tfrac{2}{3}+\tfrac{1}{3})\right|^2 = \tfrac{1}{2}\ , \\ < Q_j^2 >_\omega &= \left|\tfrac{1}{\sqrt{2}}(\tfrac{2}{3}-\tfrac{1}{3})\right|^2 = \tfrac{1}{18}\ , \\ < Q_j^2 >_\phi &= \left|\tfrac{1}{3}\right|^2 = \tfrac{1}{9}\ , \\ < Q_j^2 >_{J/\psi} &= \left|\tfrac{2}{3}\right|^2 = \tfrac{4}{9}\ . \end{aligned} \tag{5}$$

Using the property $\Gamma_{V\to e^+e^-}/ < Q_j^2 > \simeq const$ we can obtain the following approximate relations

$$m_\rho/f_\rho^2 : m_\omega/f_\omega^2 : m_\varphi/f_\varphi^2 : m_{J/\psi}/f_{J/\psi}^2 = 9:1:2:8 \tag{6}$$

which are in fairly good agreement with experimental measurements of decay widths [9].

We take into account these relations by introducing coefficients N_V (following to [10]) and writing the amplitude as $A_{\gamma p\to Vp} = N_C N_V A_{Vp\to Vp}$, where

$$N_C = 3\ ; N_\rho = \frac{1}{\sqrt{2}}\ ; N_\omega = \frac{1}{3\sqrt{2}}\ ; N_\phi = \frac{1}{3}\ ; N_{J/\psi} = \frac{2}{3}\ . \tag{7}$$

The amplitude of the process $Vp \to Vp$ may be written in the following form

$$A(z,t;M_V^2,\tilde{Q}^2) = I\!P(z,t;M_V^2,\tilde{Q}^2) + f(z,t;M_V^2,\tilde{Q}^2) + ...\ , \tag{8}$$

where, $\tilde{Q}^2 = Q^2 + M_V^2$.

$I\!P(z,t;M_V^2,\tilde{Q}^2)$ is the Pomeron contribution for which we use the so called dipole Pomeron which gives a very good description of all hadron-hadron total cross sections [11],[12]. Specifically, $I\!P$ is given by [13]

$$I\!P(z,t;M_V^2,\tilde{Q}^2) = ig_0(t;M_V^2,\tilde{Q}^2)(-iz)^{\alpha_{I\!P}(t)-1} + ig_1(t;M_V^2,\tilde{Q}^2)ln(-iz)(-iz)^{\alpha_{I\!P}(t)-1}\ , \tag{9}$$

where the first term is a single j-pole contribution and the second (with an additional $ln(-iz)$ factor) is the contribution of the double j-pole.

A similar expression applies to the contribution of the f-Reggeon

$$f(z,t;M_V^2,\tilde{Q}^2) = ig_f(t;M_V^2,\tilde{Q}^2)(-iz)^{\alpha_f(t)-1}. \tag{10}$$

It is important to stress that in this model the intercept of the Pomeron trajectory is equal to 1

$$\alpha_{I\!P}(0) = 1. \tag{11}$$

Thus the model does not violate the Froissart-Martin bound [14].

For ρ and φ meson photoproduction we write the scattering amplitude as the sum of a Pomeron and f contribution. According to the Okubo-Zweig rule, the f meson contribution should be suppressed in the production of the φ and J/ψ mesons, but given the present crudeness of the state of the art, we added the f meson contribution in the φ meson case. While we expect the f contribution to J/ψ meson production to be essentially zero, we believe that it is not irrelevant for φ meson production due to $\omega - \phi$ mixing. Indeed, in the φ decay mode, more than 15% is due to non strange particles and the $\bar{K}K$ decay mode is present in f meson decay.

For ω meson photoproduction, we include also π meson exchange (see also the discussion in [15]), which is needed in the low energy sector given that we try to describe the data for all energies W. Even though we did not expect it, the model describes well the data down to threshold.

In the integrated elastic cross section

$$\sigma(z, M_V^2, \tilde{Q}^2)_{el}^{\gamma p \to Vp} = 4\pi \int_{t_-}^{t_+} dt |A^{\gamma p \to Vp}(z, t; M_V^2, \tilde{Q}^2)|^2 \,, \tag{12}$$

the upper and lower limits

$$2t_\pm = \pm \frac{L_1 L_2}{W^2} - (W^2 + Q^2 - M_V^2 - 2M_p^2) + \frac{(Q^2 + M_p^2)(M_V^2 - M_p^2)}{W^2}, \tag{13}$$

$$L_1 = \lambda(W^2, -Q^2, M_p^2), \qquad L_2 = \lambda(W^2, M_V^2, M_p^2), \tag{14}$$

$$\lambda^2(x, y, z) = x^2 + y^2 + z^2 - 2xy - 2yz - 2zx, \tag{15}$$

are determined by the kinematical condition $-1 \leq \cos\theta_s \leq 1$ where θ_s is the scattering angle in the s-channel of the process.

The accurate account of the kinematically available t region allows us to describe effectively the threshold behaviour of cross sections, so that when $W \to W_{threshold}$ we have $t_- \to t_+$ and the elastic cross section goes to zero. The imaginary part of the amplitude does not vanish at threshold, but it turns out that the kinematical cancellation alone accounts for the threshold behaviour. The kinematical character of the threshold behaviour of the integrated cross sections was studied long ago [16].

For the Pomeron contribution (9) we use a nonlinear trajectory

$$\alpha_{I\!P}(t) = 1 + \gamma(\sqrt{4m_\pi^2} - \sqrt{4m_\pi^2 - t}\,), \tag{16}$$

where m_π is the pion mass. Such a trajectory was utilized for photoproduction amplitudes in [17], [18] and its roots are very old [19].

For the f-meson contribution for the sake of simplicity we use the standard linear Reggeon trajectory

$$\alpha_{I\!R}(t) = \alpha_{I\!R}(0) + \alpha'_{I\!R}(0)\, t \,. \tag{17}$$

In the case of nonzero virtuality of the photon, we have a new variable in play $Q^2 = -q^2$. At the same time, the cross section σ_L is nonzero. According to [4], QCD predicts the following dependence for σ_T, σ_L and their ratio as Q^2 goes to infinity:

$$\sigma_T \sim \frac{1}{Q^8}(x_{I\!P} G(x_{I\!P}, \tilde{Q}^2/4))^2;$$

$$\sigma_L \sim \frac{1}{Q^6}(x_{I\!P} G(x_{I\!P}, \tilde{Q}^2/4))^2; \tag{18}$$
$$R \equiv \sigma_L/\sigma_T \sim Q^2/M_V^2;$$
$$\sigma = (\sigma_T + \sigma_L)\Big|_{Q^2\to\infty} \sim \sigma_L.$$

Wheere $x_{I\!P} G(x_{I\!P}, \tilde{Q}^2/4)$ is the gluon distribution function and $x_{I\!P} = \frac{Q^2+M_V^2}{W^2+M_V^2}$ (see however [21, 22] where another possibility is investigated).

2 The Model

For the Pomeron resides we use the following parametrization

$$g_i(t; M_V^2, \tilde{Q}^2) = \frac{g_i}{Q_i^2 + \tilde{Q}^2} exp(b_i(t; \tilde{Q}^2)) \,, \tag{19}$$
$$i = 0, 1 \,.$$

The slopes are chosen as

$$b_i(t; \tilde{Q}^2) = \Big(b_{i0} + \frac{b_{i1}}{1 + \tilde{Q}^2/Q_b^2}\Big)(\sqrt{4m_\pi^2} - \sqrt{4m_\pi^2 - t}\,) \,, \tag{20}$$
$$i = 0, 1 \,,$$

to comply with the previous choice (16) and analyticity requirements [19].
The Reggeon residue is

$$g_{I\!R}(t; M_V^2, \tilde{Q}^2) = \frac{g_{I\!R} M_p^2}{(Q_{I\!R}^2 + \tilde{Q}^2)\tilde{Q}^2} exp(b_{I\!R}(t; \tilde{Q}^2)) \,, \tag{21}$$

where

$$b_{I\!R}(t; \tilde{Q}^2) = \frac{b_{I\!R}}{1 + \tilde{Q}^2/Q_b^2} t \,, \tag{22}$$

g_0, g_1, Q_0^2 (GeV^2), Q_1^2 (GeV^2), $Q_{I\!R}^2$ (GeV^2), Q_b^2 (GeV^2), b_{00} (GeV^{-1}), b_{01} (GeV^{-1}), b_{10} (GeV^{-1}), b_{11} (GeV^{-1}), $b_{I\!R}$ (GeV^{-2}) are adjustable parameters. $I\!R = f$ for ρ and φ, $I\!R = f, \pi$ for ω. We use the same slope $b_{I\!R}$ for f and π Reggeon exchanges.

2.1 Photoproduction of vector mesons by real photons ($Q^2 = 0$).

In the fit we use all available data starting from the threshold for each meson. As the new dataset of ZEUS [1] provides us with the unique information on both integrated elastic cross section and differential distribution of exclusive J/ψ meson photoproduction, we keep only these data for $Q^2 = 0$. This allows us to explore the effects of nonlinearity of the Pomeron trajectory and residues. In the region of non zero Q^2 the combined data of H1 and ZEUS is used.

Different experiments have different normalization especially at low energies. This implies that the χ^2/d.o.f. will not be very good while the overall agreement is quite satisfactory.

The whole set of data is composed of 357 experimental points [4] and, with a grand total of 12 parameters, we find χ^2/d.o.f = 1.49. The main contribution to χ^2 comes from the low energy region ($W \leq 4\ GeV$); had we started fitting from $W_{min} = 4\ GeV$, the resulting χ^2/d.o.f = 0.85 for the elastic cross sections would be much better and more appropriate for a high energy model.

In order to get a reliable description and the parameters of the trajectories and residues we use elastic cross sections for each process from threshold up to the highest values of the energy and differential cross sections in the whole t-region where data are available: $0 \leq |t| \leq 1.6\ GeV^2$. The data on differential cross section of ρ meson production at $W = 71.3\ GeV$ and φ meson production at $W = 13.731\ GeV$ are not included in the fitting procedure.

The parameters are given in Table 1. The errors on the parameters are obtained by MINUIT.

N	Parameter	Value	Error		Trajectory	$\alpha(0)$	$\alpha'(0)\ GeV^{-2}$
1	$\gamma\ (GeV^{-1})$	0.53853E-01	0.15666E-01			FIXED	FIXED
2	g_1	0.10435E-01	0.17851E-03	1	f Reggeon	0.8	0.85
3	g_0	-0.32901E-01	0.49449E-04	2	π Reggeon	0.0	0.85
4	g_f	0.83371E-01	0.49503E-03		Meson	# of points	χ^2 per point
5	g_π	0.60011	0.21962E-01	1	$\rho_0(770)$	σ_{el}, 127	1.49
6	$Q_0^2\ (GeV^2)$	0.0	FIXED		$\rho_0(770)$	$\frac{d\sigma_{el}}{dt}$, 24	0.99
7	$Q_1^2\ (GeV^2)$	0.41908	0.23586E-02	2	$\omega(782)$	σ_{el}, 57	1.65
8	$Q_{I\!R}^2\ (GeV^2)$	0.0	FIXED		$\omega(782)$	$\frac{d\sigma_{el}}{dt}$, 12	0.83
8	$Q_b^2\ (GeV^2)$	3.9724	0.32482	3	$\varphi(1020)$	σ_{el}, 39	0.98
10	$b_{10}\ (GeV^{-1})$	2.1251	0.73983E-01		$\varphi(1020)$	$\frac{d\sigma_{el}}{dt}$, 5	0.61
11	$b_{11}\ (GeV^{-1})$	2.5979	0.21451	4	$J/\psi(3096)$	σ_{el}, 29	0.79
12	$b_{00}\ (GeV^{-1})$	2.6967	0.24985E-01		$J/\psi(3096)$	$\frac{d\sigma_{el}}{dt}$, 70	1.92
13	$b_{01}\ (GeV^{-1})$	6.7897	0.18717E-01		All mesons	# of points	χ^2/d.o.f.
14	$b_{I\!R}\ (GeV^{-2})$	4.5741	0.10509E-02		$\rho_0, \omega, \varphi, J/\psi$	357	1.49

Table 1: Parameters obtained by fitting ρ_0, ω, φ and J/ψ photoproduction data

The results are presented in Fig. 2, which shows also the prediction of the model for $\Upsilon(9460)$ photoproduction.

As can be seen, the model describes the vector meson exclusive photoproduction data without the need of Pomeron contribution with intercept higher than 1. In addition, the rapid rise of the J/ψ cross section at low energies is described as a transition phenomenon, a delay of the onset of the real asymptotic.

Had one assumed SU(5) flavour symmetry for the $\Upsilon(9460)$, we would have found $< Q_j^2 >_\Upsilon = 1/9$ and thus $N_\Upsilon = N_\varphi$. This relation leads to underestimate the Υ photoproduction cross section (see solid line Fig. 2). Phenomenologically we find that $N_\Upsilon = N_{J/\psi}$ gives a better description of the data on $\Upsilon(9460)$ production (dotted line), but perhaps an intermediate value would be more appropriate.

[4] The data are available at
REACTION DATA Database *http://durpdg.dur.ac.uk/hepdata/reac.html*
CROSS SECTIONS PPDS database *http://wwwppds.ihep.su:8001/c1-5A.html*

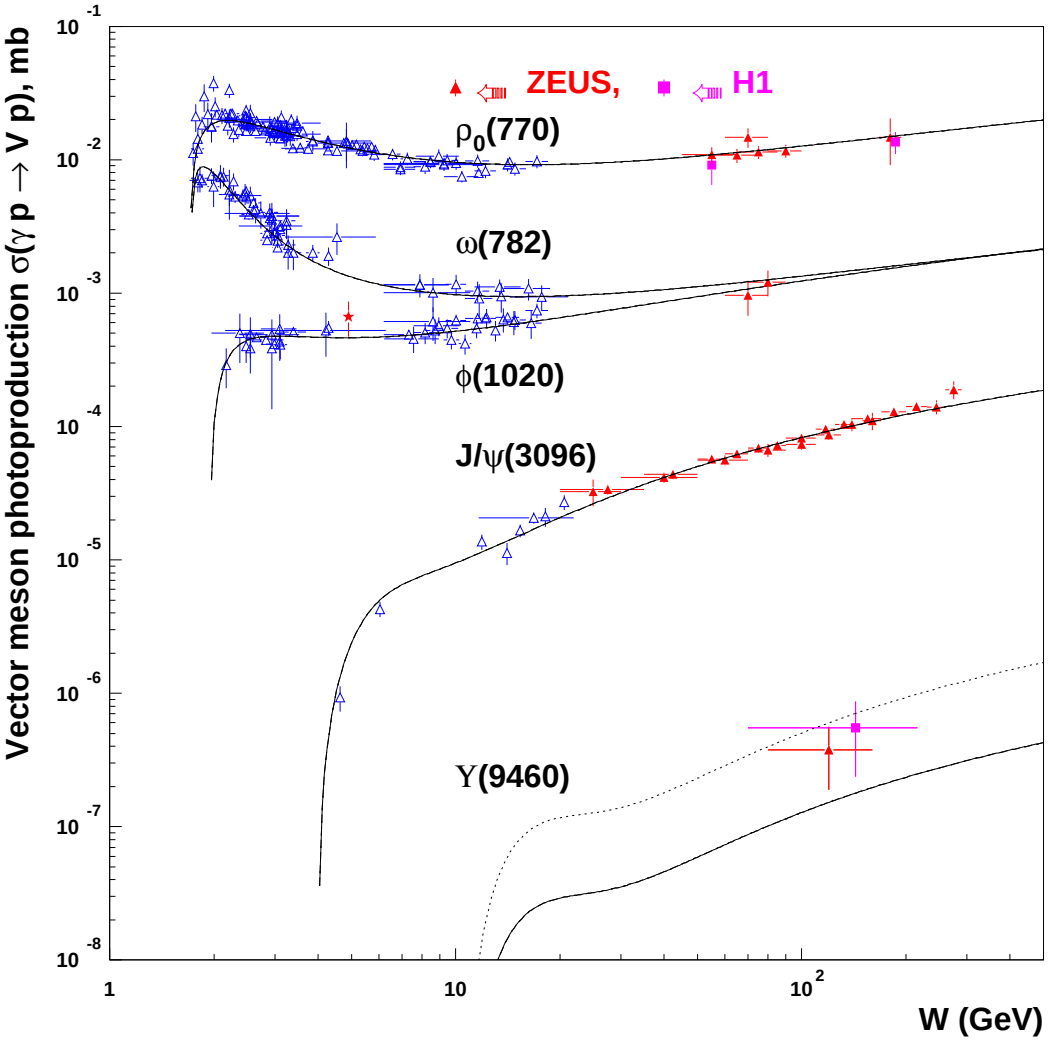

Figure 2: Elastic cross-sections for vector meson photoproduction. The solid curve for $\Upsilon(9460)$ production corresponds to $N_\Upsilon = N_\varphi$, the dotted line to $N_\Upsilon = N_{J/\psi}$.

2.2 Differential cross section of vector meson exclusive production

The differential cross section is given by

$$\frac{d\sigma}{dt} = 4\pi |A(z,t;\tilde{Q}^2, M_V^2)|^2 \ . \tag{23}$$

Using the amplitude from the previous section this quantity is now calculated and the comparison with the data is presented in Fig. 3, 4, 6, 5, 7 and 8.

Given the universality of our approach we conclude that extracting the Pomeron trajectory from the experimental data as proposed in [20] and [1] using the data depicted in Fig. 5 cannot be regarded as a valid argument to support either hard Pomeron contribution or the BFKL Pomeron.

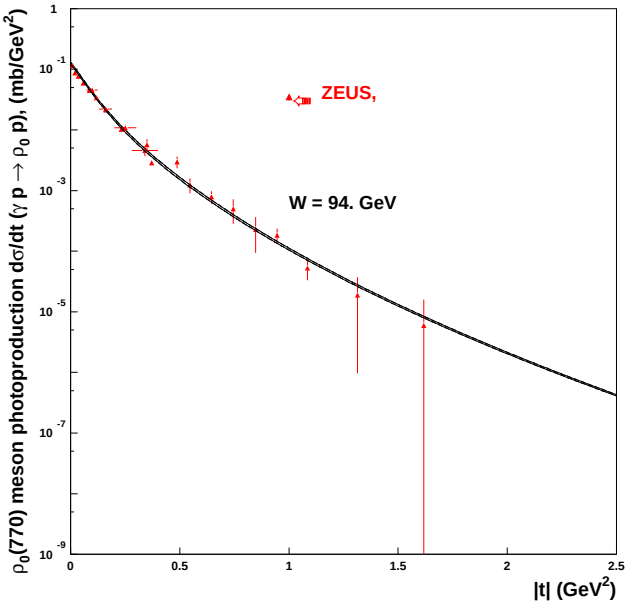

Figure 3: Differential cross section of exclusive ρ_0 meson photoproduction for $W = 94\ GeV$.

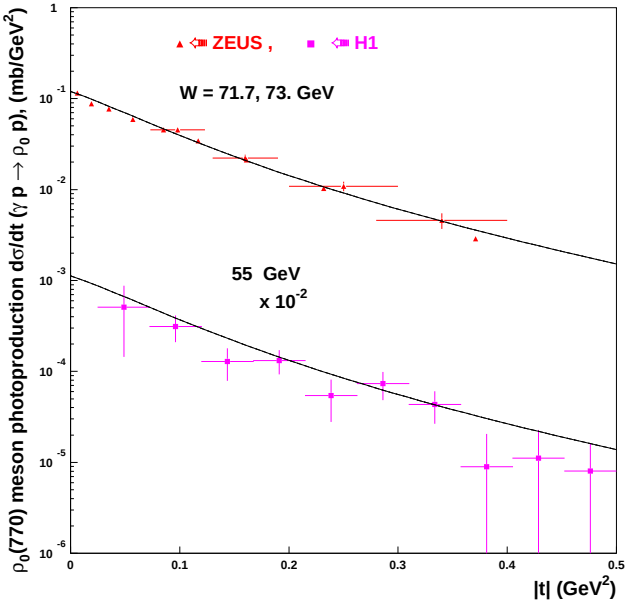

Figure 4: Differential cross section of exclusive ρ_0 meson photoproduction for $W = 71.7,\ 73,$ and $55\ GeV$. The data and curves for $W = 55\ GeV$ are scaled by a factor 10^{-2}.

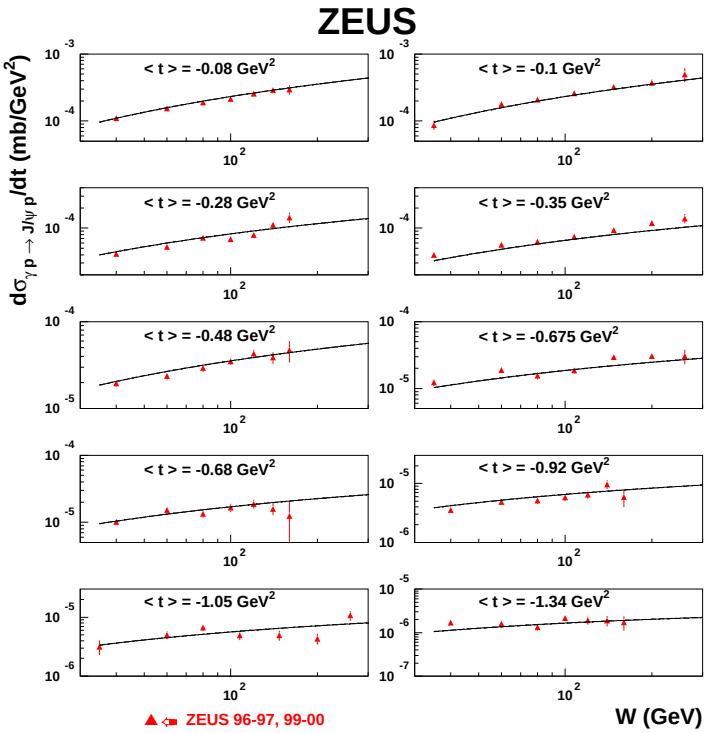

Figure 5: Differential cross section of exclusive J/ψ meson photoproduction as a function of W at different $< t >$.

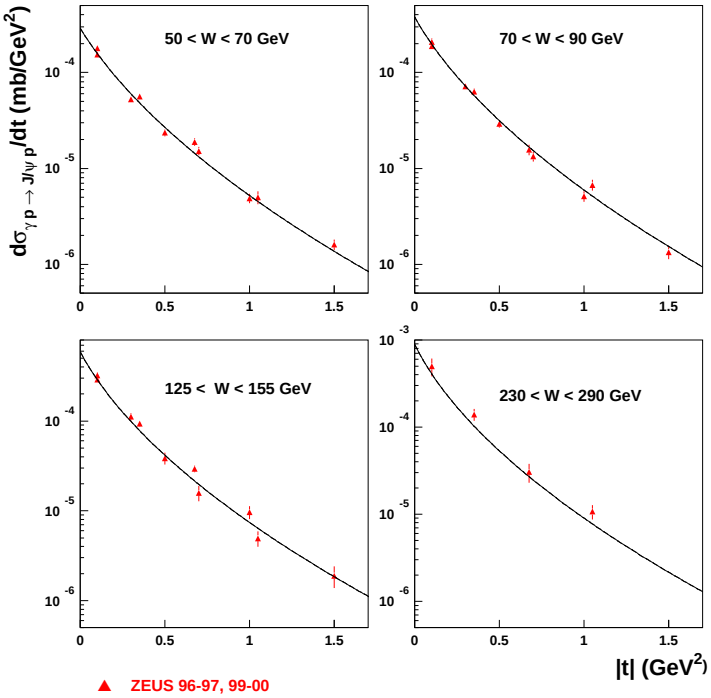

Figure 6: Differential cross section of exclusive J/ψ meson photoproduction.

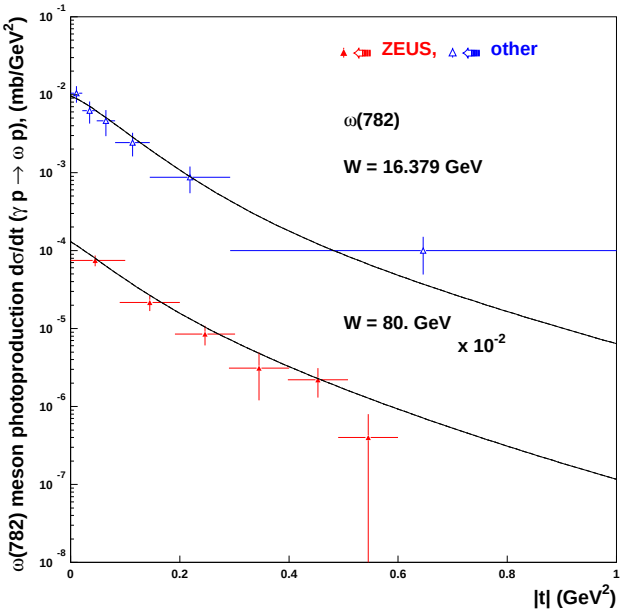

Figure 7: Differential cross section of exclusive ω meson photoproduction for $W = 16.379$ and 80 GeV. The data and curves for $W = 80$ GeV are scaled by a factor 10^{-2}.

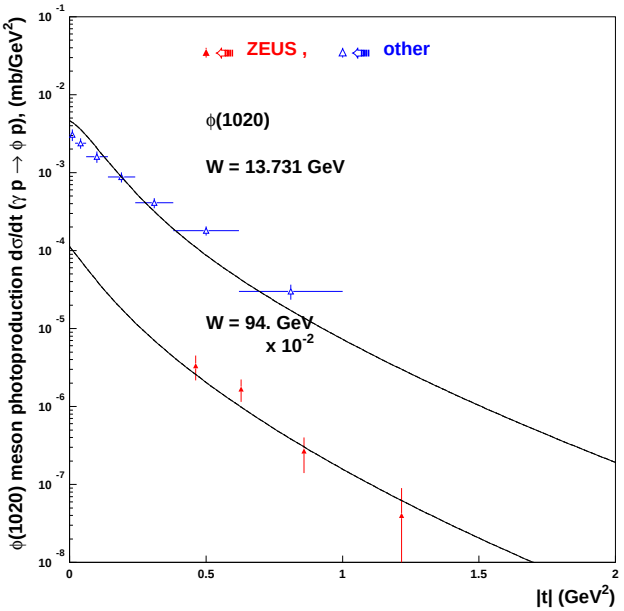

Figure 8: Differential cross section of exclusive φ meson photoproduction for $W = 13.371$ and 94 GeV. The data and curves for $W = 94$ GeV are scaled by a factor 10^{-2}.

Exploring the nonlinearity of the Pomeron trajectory (16) and slopes (19), we have tried adding to either a linear term or a heavier threshold; both give negligibly small effects. Thus

we conclude that new ZEUS data on $d\sigma_{J/\psi}/dt$ (see for example Fig. 6) are a strong support in favor of the nonlinear Pomeron trajectory.

2.3 Photoproduction of vector mesons by virtual photons ($Q^2 > 0$).

In (19) and (21) the Q^2- dependence ($\tilde{Q}^2 = Q^2 + M_V^2$) is completely fixed up to an *a priori* arbitrary dimensionless function $f(Q^2)$ such that $f(0) = 1$. Thus, we may introduce a new factor that differentiates virtual from real photoproduction:

$$f(Q^2) = \Big(\frac{M_V^2}{\tilde{Q}^2}\Big)^n \tag{24}$$

Accordingly, in the case $Q^2 \neq 0$ we use the following parametrizations for Pomeron couplings (compare with Eq. 19):

$$\hat{g}_i(t; \tilde{Q}^2, M_V^2) = f(Q^2) g_i(t; \tilde{Q}^2, M_V^2),\ i = 0, 1, \tag{25}$$

where, for the sake of completeness, we will examine three different *choices* for the asymptotic Q^2 behaviour of the Pomeron residue

Choice I

$$n = 1, \qquad \sigma_T(Q^2 \to \infty) \sim \frac{1}{Q^8}\ . \tag{26}$$

Choice II

$$n = 0.5, \qquad \sigma_T(Q^2 \to \infty) \sim \frac{1}{Q^6}\ . \tag{27}$$

Choice III

$$n = 0.25, \qquad \sigma_T(Q^2 \to \infty) \sim \frac{1}{Q^5}\ . \tag{28}$$

For the reggeon couplings we have

$$f_{I\!R}(Q^2) = \Big(\frac{c_1 M_V^2}{c_1 M_V^2 + Q^2}\Big)^{n_2}\ , \tag{29}$$

where c_1 is an adjustable parameter and $n_2 = 0.25,\ -0.25,\ -0.5$ for *choice I, II, III*.

Accordingly, in the case $Q^2 \neq 0$ we use the following parametrizations for Reggeons couplings (compare with Eq. 21):

$$\hat{g}_{I\!R}(t; \tilde{Q}^2, M_V^2) = f_{I\!R}(Q^2) g_{I\!R}(t; \tilde{Q}^2, M_V^2)\ . \tag{30}$$

The lack of data on the ratio σ_L/σ_T, especially in the high Q^2 domain, does not allow us to draw definite conclusions about its asymptotic behaviour (the Regge theory is not the appropriate tool for giving predictions in this case), nor do we have a unique prescription in the framework of our model. There may be several realizations of the model with different asymptotic behaviour of σ_L/σ_T [2]. As a demonstration of such a possibility we explore the predictions (18) and use the following (most economical) parametrization for R (which cannot be deduced from the Regge theory)

Choice I, II, III

$$R(Q^2, M_V^2) = \Big(\frac{cM_V^2 + Q^2}{cM_V^2}\Big)^{n_1} - 1 \tag{31}$$

where c and n_1 are adjustable parameters for *choice I, II, III.*

We have, thus, 3 additional adjustable parameters as compared with real photoproduction. In order to obtain the values of the parameters for the case $Q^2 \neq 0$, we fit just the data[5] on ρ_0 meson photoproduction in the region $0 \leq Q^2 \leq 35\ GeV^2$; the parameters for photoproduction by real photons are the same as in Table 1. In order to avoid the low W region where nucleon resonances may spoil the picture of ρ meson exclusive production, we restrict ourselves to the energy domain $W \geq 4\ GeV$ for $Q^2 \neq 0$.

The parameters thus obtained are shown in Table 2.

		Choice I	*Choice II*	*Choice III*
N	Parameter	Value	Value	Value
1	c	1.2666 ± 0.048	1.6900 ± 0.167	3.3282 ± 0.916
2	n_1	1.8355 ± 0.026	0.84596 ± 0.033	0.32453 ± 0.043
3	c_1	2.3258 ± 0.286	0.55469 ± 0.044	0.78464 ± 0.028
	Fit, # of points	χ^2/d.o.f.	χ^2/d.o.f.	χ^2/d.o.f.
	$\rho_0(770)$, 283	1.47	1.53	1.56
	Meson, # of points	χ^2 per point	χ^2 per point	χ^2 per point
1	ρ_0, 283	1.45	1.51	1.54
2	ω, 67	1.46 **(no fit!)**	1.46 **(no fit!)**	1.46 **(no fit!)**
3	φ, 56	0.78 **(no fit!)**	0.79 **(no fit!)**	0.82 **(no fit!)**
2	J/ψ, 54	0.89 **(no fit!)**	0.92 **(no fit!)**	0.99**(no fit!)**

Table 2: Parameters obtained by fitting ρ_0 virtual photoproduction data for *choice I, II, III.*

The results of the fit are depicted in Figs. 9, 10, 11, 12. In these figures as well as in all following ones the solid lines, dashed lines and dotted lines correspond to the *choice I, II, III* correspondingly. The description of the data is very good at all energies. Both high energy data from ZEUS and H1 Fig. 9 and low energy data from HERMES Fig. 11 are accounted for. In the region of the HERMES data (Fig. 11) our description is comparable to the one of Haakman, Kaidalov and Koch [23] (see [24] for details).

[5]The data are available at
REACTION DATA Database *http://durpdg.dur.ac.uk/hepdata/reac.html*
CROSS SECTIONS PPDS database *http://wwwppds.ihep.su:8001/c1-5A.html*

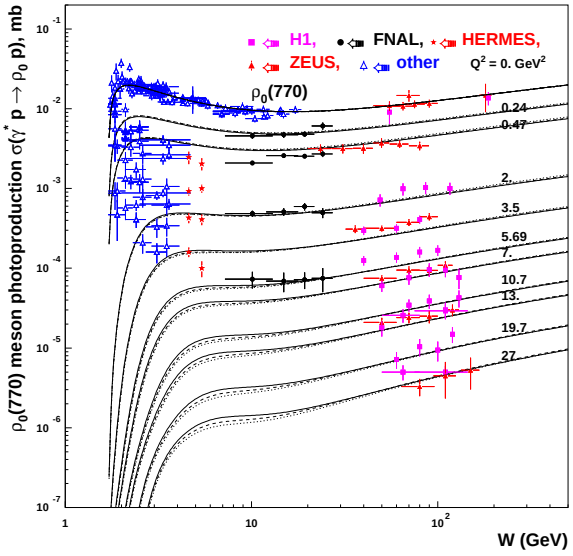

Figure 9: Elastic cross section of exclusive ρ_0 virtual photoproduction as a function of W for different values of Q^2.

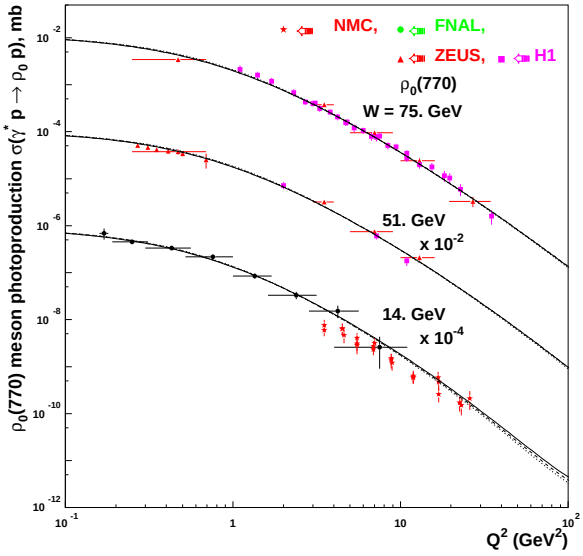

Figure 10: Elastic cross section of exclusive ρ_0 virtual photoproduction as a function of Q^2 for $W = 75,\ 51,$ and $14\ GeV$. The data and curves for $W = 51,$ and $14\ GeV$ are scaled by factors 10^{-2} and 10^{-4}.

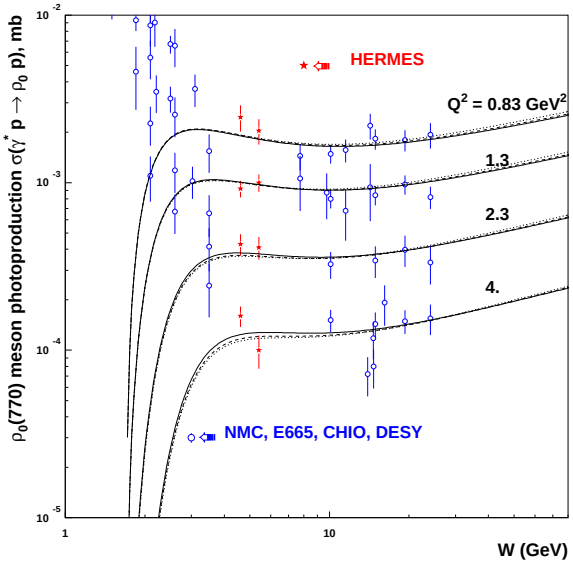

Figure 11: Elastic cross section of exclusive ρ_0 virtual photoproduction as a function of W for various Q^2 in the region of low and intermediate W.

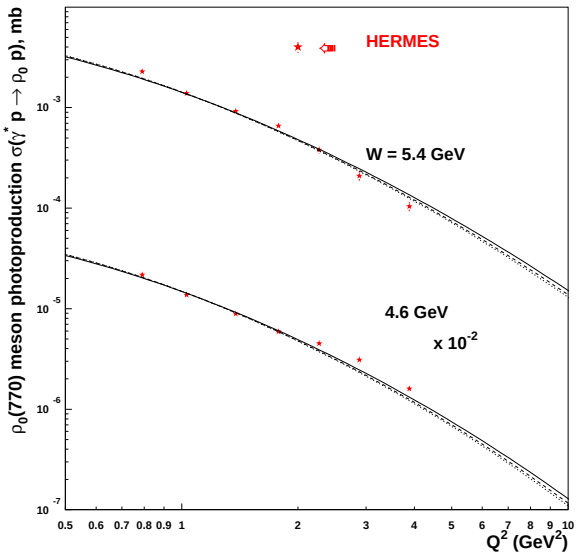

Figure 12: Elastic cross section of exclusive ρ_0 virtual photoproduction as a function of Q^2 for $W = 5.4,$ and $4.6\ GeV$. The data and curves for $W = 4.6\ GeV$ are scaled by a factor 10^{-2}.

We can now check the predictions of the model. As stated earlier, we aim at a unified

model for all vector meson production, thus the only variable that changes is the mass of the vector meson. In the following figures we depict our *predictions* for ω, φ and J/ψ mesons and we compare them with the available data. The *description* of the data is very good for all the three mesons. The $\chi^2 = 0.89$ for J/ψ meson exclusive production follows without any fitting. Both W and Q^2 dependences are reproduced very well. Notice that, so far, the three *choices I, II, III* all give equally acceptable reproduction of the data.

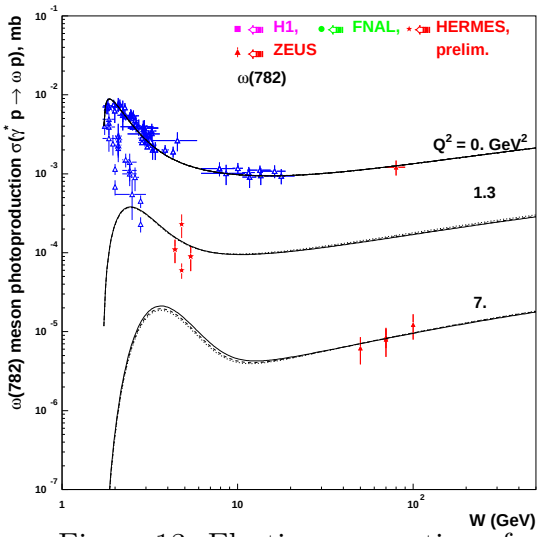

Figure 13: Elastic cross section of exclusive ω virtual photoproduction as a function of W for various Q^2.

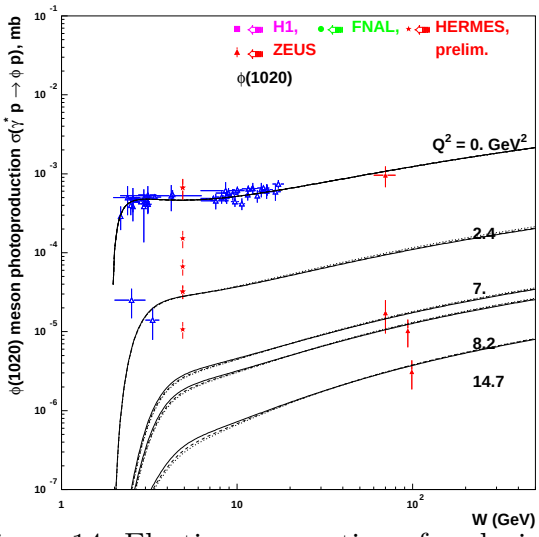

Figure 14: Elastic cross section of exclusive φ virtual photoproduction as a function of W for various Q^2.

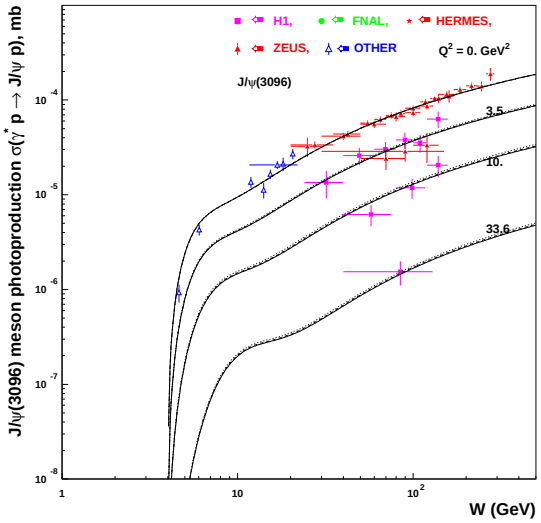

Figure 15: Elastic cross section of exclusive J/ψ virtual photoproduction as a function of W for various Q^2.

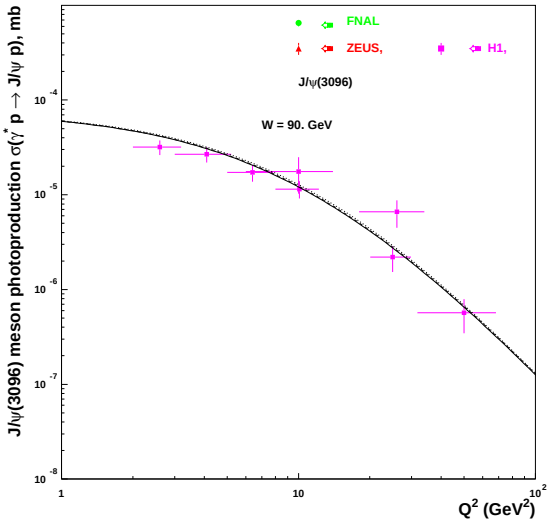

Figure 16: Elastic cross section of exclusive J/ψ virtual photoproduction as a function of Q^2 for $W = 90\ GeV$.

We now plot the various ratios σ_L/σ_T (these data were not fitted) corresponding to Eqs (26),(27),(28) (shown with the solid (*choice I*), dashed (*choice II*) and dotted (*choice III*) lines) in Fig. 17, 18, 19. The result shows, indeed, a rapid increase of σ_L/σ_T with increasing Q^2, however one can see that our intermediate *choice II* is preferable to either *I* or *III* on this basis.

Let us examine the obtained dependences. We find that the data prefer

$$R(Q^2 \to \infty) \sim \left(\frac{Q^2}{M_V^2}\right)^{n_1}, \tag{32}$$

where $n_1 \simeq 2,\ 1,\ 0.3$ in *choice I, II and III*. Our, probably oversimplified, estimates and the data show $0.3 < n_1 < 1$, see Fig. 17, thus $\sigma \sim 1/Q^N$ where $N \in (4, 4.4)$ as $N = 6 - 2n_1$ for the *choice II* and $N = 5 - 2n_1$ for the *choice III*. However it is evident that new more precise data on R are need.

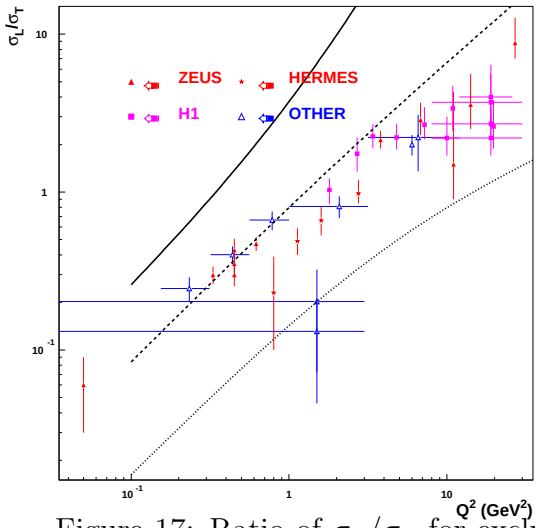

Figure 17: Ratio of σ_L/σ_T for exclusive ρ_0 large Q^2 photoproduction.

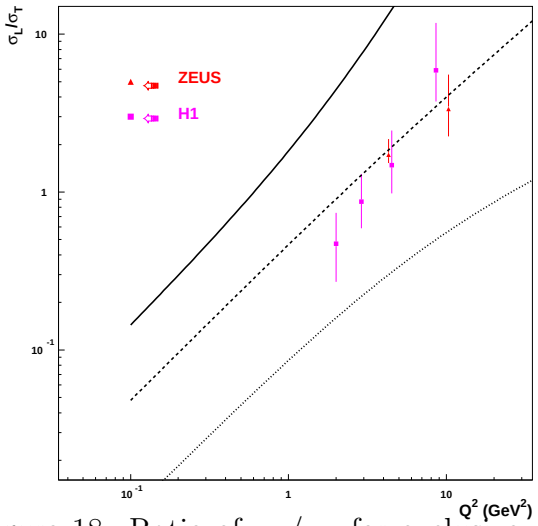

Figure 18: Ratio of σ_L/σ_T for exclusive φ large Q^2 photoproduction.

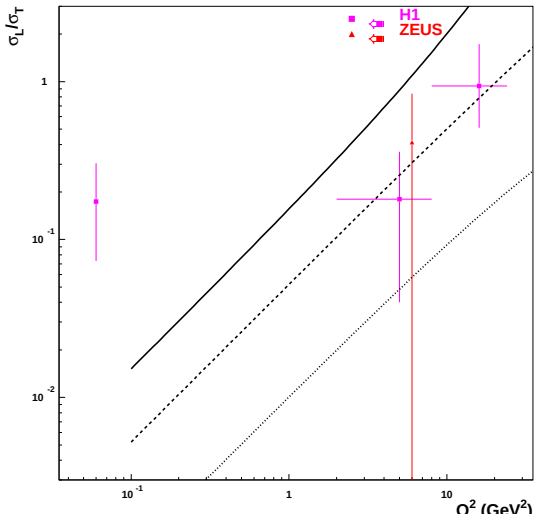

Figure 19: Ratio of σ_L/σ_T for exclusive J/ψ large Q^2 photoproduction.

3 Conclusion

We have shown that minor changes in the Soft Dipole Pomeron model recently developed [2] for vector meson photoproduction allow us to describe well the new ZEUS data [1] on the differential and integrated cross-sections for $\gamma p \to J/\psi p$. Again, all available data on photoproduction of other vector mesons at $Q^2 = 0$ as well as $Q^2 \neq 0$ are well reproduced.

The changes made do not affect the main properties of the model such as: (i) the Pomeron intercept which is equal to one, (ii) the hardness of the Pomeron, *i.e.* the fact that it is a double pole in the complex j-plane.

We take directly into account the kinematical limits through the variable $z \propto \cos\theta_t$. The nonlinear Pomeron trajectory $\alpha_P(t) = 1 + \gamma\,(\sqrt{4m_\pi^2} - \sqrt{4m_\pi^2 - t})$ turns out to be more suitable for the nonlinearity of the diffractive cone shown by the new ZEUS data. This is not unexpected as the linear behaviour of the $I\!P$ trajectory is hard to reconcile with analyticity. We have implemented also the correct limits of t-integration. The last circumstance allows us to account for the threshold behaviour of the cross-sections.

We would like to emphasize the following important points (confirming the main findings of [2] and repeating some of them)

1. The new ZEUS data [1] (in contrast to the old ones) quite definitely point towards the nonlinearity of the Pomeron slope and trajectory.

2. Our model describes the data also at low energies due to the kinematical shrinkage of the available t region. This is particularly important for J/ψ production where the bulk of the available data is not so far from its threshold.

3. Phenomenologically we find that in the region of available Q^2 the ratio $\sigma_L/\sigma_T \sim (Q^2/M_V^2)^{n_1}$, where $0.3 < n_1 < 1$. The definite conclusion can be derived only with new precise data on the ratio σ_L/σ_T, especially for high Q^2.

4. Pomeron and secondary Reggeons appear as universal objects in Regge theory [7]. The corresponding j-singularities of the γ p amplitudes and their trajectories are universal. They do not depend on the properties of the external particles and, consequently, on Q^2 (only residues or vertex functions may depend on Q^2). We believe that the unitarity restrictions on the Pomeron contribution obtained strictly for the hh case must hold also for γh if it is universal.

5. The growth with energy of hadronic total cross sections and the restriction on the Pomeron intercept ($\alpha_{I\!P}(0) \leq 1$) implied by the Froissart-Martin bound [14] imply that the Pomeron is a more complicated singularity than a simple pole with $\alpha_{I\!P}(0) = 1$. We have considered the simplest case when the Pomeron is a double j-pole leading to $\sigma(s) \propto \ln s$. We have shown that one does not need a contribution with $\alpha(0) > 1$ (hard Pomeron) violating unitarity in order to describe the exclusive photoproduction data in the present region of Q^2 and t.

Acknowledgement

We would like to thank Michele Arneodo, Alexander Borissov, Jean-Rene Cudell and Alessia Bruni for various and fruitful discussions. One of us (E.M.) would like to thank the Department of Theoretical Physics of the University of Torino for its hospitality and financial support during his visit to Turin.

References

[1] ZEUS Collaboration: S. Chekanov *et al.*, *Eur.Phys.J.* C **24**, 345 (2002).

[2] E.Martynov, A.Prokudin, E.Predazzi, hep-ph/0112242, submitted to *Eur.Phys.J.* C.

[3] V. N. Gribov, B. L. Ioffe and I. Ya. Pomeranchuk, *Yad. Fiz.* **2**, 768 (1965);
B. L. Ioffe, *Phys. Lett.* B **30**, 123 (1968).

[4] S. J. Brodsky, L. Frankfurt, J. F. Gunion, A. H. Mueller and M. Strikman *Phys. Rev.* D **50**, 3134 (1994).

[5] J. R. Cudell, A. Donnachie, P. V. Landshoff, *Phys. Lett.* B **448**, 281 (1999).

[6] P.Desgrolard, E.Martynov, *Eur.Phys.J.* C **22**, 479-492 (2001).

[7] For a recent update on the Regge theory, see:
V. Barone, E. Predazzi *"High-Energy Particle Diffraction"*, Springer-Verlag Berlin Heidelberg (2002)

[8] J.J. Sakurai, *Ann. Phys. NY* **11**,1 (1960);
M. Gell-Mann and F. Zacharaisen, *Phys. Rev.* D **124**, 953 (1961).

[9] D.E. Groom *et al. Eur.Phys.J.* C **15**, 1 (2000).

[10] J. Nemchik, N. N. Nikolaev, E. Predazzi and B. G. Zakharov *Z. Phys.* C **75**, 71 (1997).

[11] P.Desgrolard, M.Giffon, A.Lengyel, E.S.Martynov, *Nuovo Cimento* **107**, 637 (1994).

[12] J.R.Cudell *et al.*, COMPETE Collaboration, *Phys. Rev.* D **65**, 074024 (2002).

[13] E.S.Martynov, *Unitarization of Pomeron and Regge Phenomenology of Deep Inelastic Scattering.* Proceedings of Workshop "Hadrons-94".
Kiev,1994; Preprint ITP-94-49E, Kiev, 1994;
L.Jenkovszky, E.Martynov and F.Paccanoni, *"Regge behaviour of the nucleon structure function"*, Padova preprint, DFPD 95/TH/21.

[14] M. Froissart, *Phys. Rev.* D **123**, 1053 (1961);
A. Martin, *Phys. Rev.* D **129**, 993 (1963).

[15] A. Donnachie, P. V. Landshoff, *Phys. Lett.* B **185**, 403 (1987);
A. Donnachie, P. V. Landshoff, *Phys. Lett.* B **348**, 213 (1995).

[16] L. Fonda and R. G. Newton, *Nuovo Cimento* **14**, 1027 (1959).

[17] L.L. Jenkovszky, E.S.Martynov, F.Paccanoni *"Regge Pole Model for Vector Meson Photoproduction at HERA"*, hep-ph/9608384.

[18] R. Fiore, L. L. Jenkovszky, F. Paccanoni *Eur.Phys.J.* C **10**, 461 (1999); R. Fiore, L. L. Jenkovszky, F. Paccanoni, A. Papa *"Soft J/ψ photoproduction at HERA"*, hep-ph/0110405.

[19] E. Predazzi, *Ann. of Phys. (NY)* **36**, 250 (1966).

[20] H1 Collaboration: C.Adloff, et al *Phys. Lett.* B **483**, 23 (2000).

[21] J.R. Cudell and I. Royen *Phys. Lett.* B **397**, 317 (1997).

[22] J.R. Cudell and I. Royen *Nucl. Phys.* B **545**, 505 (1999).

[23] L.P.A. Haakman, A. Kaidalov and J. H. Koch, *Phys. Lett.* B **365**, 411 (1996).

[24] HERMES Collaboration: Airapetian, *et al*, *Eur.Phys.J.* C **17**, 389 (2000).